Graphical peak analysis method for determining densities and emission rates of traps in dielectric film from transient discharge current

Hideharu Matsuura,[a] Takashi Hase, Yasuhiro Sekimoto, and Masaharu Uchikura
Department of Electronics, Osaka Electro-Communication University, 18-8 Hatsu-cho, Neyagawa, Osaka 572-8530, Japan

Masaru Simizu
Department of Electronics, Himeji Institute of Technology, 2167 Shosha, Himeji, Hyogo 671-2201, Japan

(Received 4 June 2001; accepted for publication 30 October 2001)

The purpose of this study is to propose and test the graphical peak analysis method [discharge current transient spectroscopy (DCTS)] for determining the densities and emission rates of traps in a dielectric thin film from the transient discharge current $I_{dis}(t)$ in a capacitor at a constant temperature, different from thermally stimulated current (TSC). It is theoretically demonstrated that DCTS can distinguish among traps with close emission rates. Experimentally, the densities and emission rates of five traps in $Pb(Zr, Ti)O_3$ thin films are determined using DCTS. Here, these five emission rates are between 1×10^{-3} s^{-1} and 7×10^{-2} s^{-1}. One kind of trap, which was determined by TSC under the assumption of one emission rate, is found to be distinguished into five kinds of traps with close emission rates by DCTS. © *2002 American Institute of Physics.* [DOI: 10.1063/1.1429768]

I. INTRODUCTION

Dioxide silicon (SiO_2) has played an important role in the performance characteristics of large scaled integrated circuits. In order to enlarge the capacitance of the capacitor in memory element cells in dynamic random access memories (DRAMs) or to reduce an operating voltage of field-effect transistors, it is now desired to make use of insulators (i.e., dielectrics) with high dielectric constants. When these dielectric thin films are used in DRAMs, the leakage currents related to traps in the films lower their performance. For the nonvolatile memory cells, on the other hand, ferroelectric random access memories (FRAMs) have been investigated.[1] However, the fatigues and imprints in FRAMs are considered to be related to traps in ferroelectric thin films.[2–5] This is why a method for precisely determining the densities and emission rates of traps in dielectric thin films is strongly required.

There are transient capacitance methods for determining the densities and energy levels of traps, for example, deep level transient spectroscopy,[6] isothermal capacitance transient spectroscopy (ICTS)[7,8] for low-resistivity semiconductors, and the heterojunction-monitored capacitance (HMC) method[9,10] for high-resistivity semiconductors such as undoped hydrogenated amorphous silicon whose resistivity is approximately 10^9 Ω cm. In the case of applying the transient capacitance methods to metal-insulator-semiconductor diodes, mainly traps at the insulator/semiconductor interface can be investigated.[11,12] However, it is difficult to determine the densities and energy levels of traps in insulator.

Thermally stimulated current (TSC) is suitable for evaluating the densities and energy levels of traps with one thermionic emission rate or with completely different thermionic emission rates in insulator.[13,14] However, TSC is available only in the case of thermionic emission processes, and it is difficult to analyze the experimental TSC data when it happens that traps with close emission rates are included in the film. Moreover, since the influence of the pyroelectric currents and the temperature dependence of the steady-state leakage currents must be considered when the measurement temperature increases continuously, an isothermal measurement is more suitable for evaluating the densities and emission rates of traps than TSC.

Although the densities and emission rates of traps can be obtained by numerical calculation of curve fitting of the transient discharge current at a constant temperature, you should assume the number of trap species before the curve-fitting procedure, indicating that the densities and emission rates of traps strongly depend on the assumed number of trap species. Moreover, in the curve-fitting procedure, the too many curve-fitting parameters (densities and emission rates) should be changed at the same time, suggesting that the obtained values should be less reliable.

Without any assumption of the number of trap species, on the other hand, one of the authors has proposed and tested a graphical peak analysis method for determining the densities and emission rates of traps using the isothermally measured transient discharge current, referred to as discharge current transient spectroscopy (DCTS).[15–19] From each peak of the DCTS signal, the density and emission rate of the corresponding trap can be determined accurately. Using DCTS, the densities and energy levels of traps in silicon nitride thin films were experimentally investigated.[15,16] However, it was difficult to distinguish among traps with close emission rates in them.

In this study, in order to distinguish among traps with close emission rates, we have improved our method.[20] After

[a]Electronic mail: matsuura@isc.osakac.ac.jp

the improved DCTS is theoretically discussed, DCTS is experimentally applied to thin films of $Pb(Zr, Ti)O_3$, called PZT.

II. DISCHARGE CURRENT TRANSIENT SPECTROSCOPY

A. Basic idea

In graphical peak analysis methods, it is desired that functions to be evaluated have a peak value N_{ti} at a peak discharge time

$$t_{\mathrm{peak}i}=\frac{1}{e_{ti}}, \tag{1}$$

where N_{ti} and e_{ti} are the density per unit area and emission rate of the ith trap, respectively. One of the functions that satisfy the condition mentioned above is expressed as[15–17]

$$D(t)=\sum_{i=1} N_{ti}e_{ti}t\exp(-e_{ti}t+1), \tag{2}$$

where t is the discharge time. Here, when traps are confirmed to be uniformly distributed in the direction of the film thickness, the density per unit volume can be calculated as N_{ti} over the film thickness. The similar basic idea has been adopted in the transient capacitance methods, that is, ICTS for low-resistivity semiconductors[8] and the HMC method for high-resistivity semiconductors.[9,10] Moreover, it has been adopted in free carrier concentration spectroscopy (FCCS), which determines the densities and energy levels of donors or acceptors in semiconductors using the temperature dependence of the majority-carrier concentration obtained from Hall-effect measurements.[21–26]

As is clear from Eq. (1), all peaks of Eq. (2) do not appear in the time range of the measurement. When we can introduce a function in which each peak appears at

$$t_{\mathrm{peak}i}=\frac{1}{e_{ti}+e_{\mathrm{ref}}}, \tag{3}$$

we can shift the peak discharge time to the measurement time range by changing the parameter (e_{ref}). This indicates that we can determine N_{ti} and e_{ti} in a wide emission-rate range, even when the measurement time range is limited. The function that satisfies this condition is

$$D(t,e_{\mathrm{ref}})=\sum_{i=1} N_{ti}e_{ti}t\exp[-(e_{ti}+e_{\mathrm{ref}})t+1]. \tag{4}$$

In this case, each peak value is

$$D(t_{\mathrm{peak}i},e_{\mathrm{ref}})=N_{ti}(1-e_{\mathrm{ref}}t_{\mathrm{peak}i}) \tag{5}$$

at $t_{\mathrm{peak}i}$ expressed as Eq. (3). Therefore, using $t_{\mathrm{peak}i}$ and $D(t_{\mathrm{peak}i},e_{\mathrm{ref}})$, the values of N_{ti} and e_{ti} can be determined as

$$N_{ti}=\frac{D(t_{\mathrm{peak}i},e_{\mathrm{ref}})}{1-e_{\mathrm{ref}}t_{\mathrm{peak}i}} \tag{6}$$

and

$$e_{ti}=\frac{1}{t_{\mathrm{peak}i}}-e_{\mathrm{ref}}, \tag{7}$$

respectively. One of the authors has already applied the similar basic idea to FCCS, while this basic idea can be easily applied to ICTS and the HMC method, in order to distinguish among traps with close emission rates.

In order to obtain Eq. (4), we define the function to be evaluated as

$$D(t,e_{\mathrm{ref}})\equiv\frac{t}{qS}[I_{\mathrm{dis}}(t)-I_{\mathrm{l}}(V_{\mathrm{dis}})]\exp(-e_{\mathrm{ref}}t+1), \tag{8}$$

where $I_{\mathrm{l}}(V_{\mathrm{dis}})$ is the steady-state leakage current at the discharge voltage (V_{dis}), q is the electron charge, and S is the electrode area.

In the case of thermionic emission processes, the energy level (ΔE_{ti}) of the ith trap, measured from the extended states, can be determined from the temperature dependence of e_{ti}, since e_{ti} is given by

$$e_{ti}=\nu_{ti}\exp\left(-\frac{\Delta E_{ti}}{kT}\right), \tag{9}$$

where ν_{ti} is the attempt-to-escape frequency and k is the Boltzmann constant.

When the time dependence of the depolarization of the ith dipole in a dielectric film is given by

$$\exp\left(-\frac{t}{\tau_i}\right), \tag{10}$$

the polarization (P_i) and relaxation time (τ_i) of the ith dipole can be determined using DCTS. In this case, e_{ti} and N_{ti} in Eq. (4) should be replaced by $1/\tau_i$ and P_i/q, respectively.[17]

B. Theoretical consideration

A capacitor, consisting of a dielectric thin film between two electrodes, is considered. When a charge voltage (V_{cha}) is applied to the capacitor in the interval of $-t_{\mathrm{cha}}<t<0$, a charge current (I_{cha}), which fills traps with charged carriers (electrons or holes), flows through the capacitor. By $t=0$, all the traps are assumed to capture charged carriers, indicating that at $t=0$ the density per unit area, $n_{ti}(t)$, of charged carriers captured at the ith trap is expressed as

$$n_{ti}(0)=N_{ti}. \tag{11}$$

At $t=0$, the applied voltage is changed from V_{cha} to V_{dis}, where V_{dis} is the discharge voltage at which the transient discharge current is measured, and $|V_{\mathrm{dis}}|<|V_{\mathrm{cha}}|$. Since the resistance in the external measurement circuit is very low, the charge due to the geometric capacity disappears in a very short time. At $t>0$, therefore, the measured $I_{\mathrm{dis}}(t)$ arises due to the emission of charged carriers from traps as well as due to the steady-state leakage current.

Since $n_{ti}(t)$ follows the rate equation

$$\frac{\mathrm{d}n_{ti}(t)}{\mathrm{d}t}=-n_{ti}(t)e_{ti}, \tag{12}$$

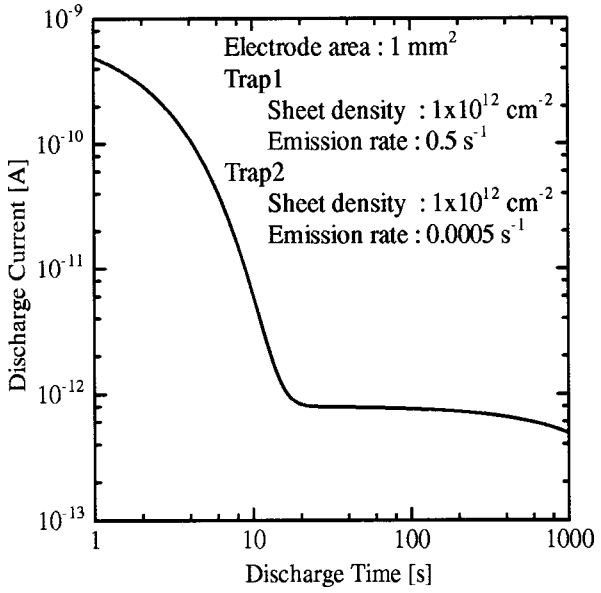

FIG. 1. Transient discharge current simulated assuming the following two kinds of traps. The sheet density and emission rate of Trap1 are 1×10^{12} cm^{-2} and 0.5 s^{-1}, respectively, and those of Trap2 are 1×10^{12} cm^{-2} and 0.0005 s^{-1}, respectively.

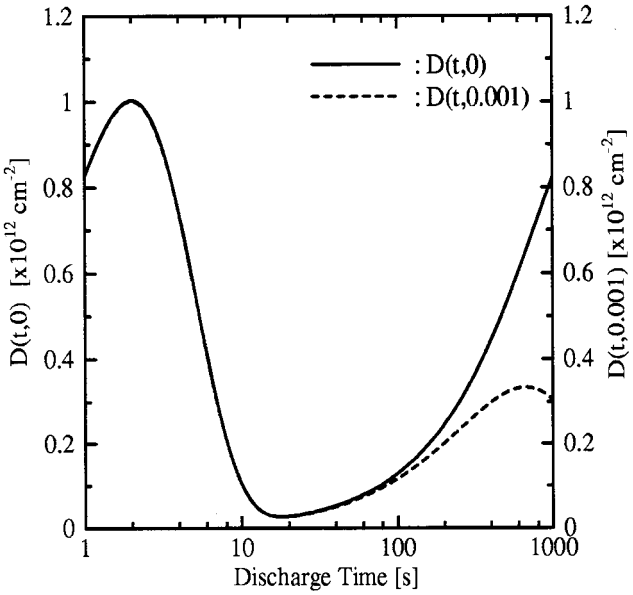

FIG. 2. DCTS signals with $e_{\mathrm{ref}}=0\ \mathrm{s}^{-1}$ (full curve) and with $e_{\mathrm{ref}}=0.001\ \mathrm{s}^{-1}$ (broken curve).

the total charge, $Q(t)$, in the film is expressed as

$$Q(t)=qS\sum_{i=1} n_{ti}(t) \tag{13}$$

$$=qS\sum_{i=1} N_{ti}\exp(-e_{ti}t). \tag{14}$$

Because the decrease of $Q(t)$ results in the transient discharge current,

$$I_{\mathrm{dis}}(t)=-\frac{\mathrm{d}Q(t)}{\mathrm{d}t}+I_{\mathrm{l}}(V_{\mathrm{dis}}). \tag{15}$$

From Eq. (8), $D(t,e_{\mathrm{ref}})$ is theoretically expressed as

$$D(t,e_{\mathrm{ref}})=\sum_{i=1} N_{ti}e_{ti}t\exp[-(e_{ti}+e_{\mathrm{ref}})t+1]. \tag{16}$$

As is clear from Eq. (16), we have obtained a suitable function for the graphical peak analysis method.

C. Shift of peak discharge time to measurement time range

It is demonstrated that e_{ref} in Eq. (8) is a useful parameter when the time range of the measurement is limited. Figure 1 shows the transient discharge current, which is simulated assuming the following two kinds of traps. N_{t1} and e_{t1} of Trap1 are 1×10^{12} cm^{-2} and 0.5 s^{-1}, respectively, and N_{t2} and e_{t2} of Trap2 are 1×10^{12} cm^{-2} and 0.0005 s^{-1}, respectively. The value of S is 1 mm^2.

Figure 2 shows the DCTS signals. The full curve represents the DCTS signal with $e_{\mathrm{ref}}=0\ \mathrm{s}^{-1}$. In this case, only one peak is detected, and the peak discharge time and peak value are 2.00 s and 1.00×10^{12} cm^{-2}, respectively. From Eqs. (6) and (7), N_{t1} and e_{t1} are determined to be 1.00×10^{12} cm^{-2} and 5.00×10^{-1} s^{-1}, respectively. Since the other peak is not detected when $e_{\mathrm{ref}}=0\ \mathrm{s}^{-1}$, however, it is impossible to determine N_{t2} and e_{t2}.

The broken curve in Fig. 2 represents the DCTS signal with $e_{\mathrm{ref}}=0.001\ \mathrm{s}^{-1}$. In this case, two peaks appear in the figure, and the two peak discharge times are 2.00 and 667 s. Using Eqs. (6) and (7), therefore, N_{t1} and e_{t1} of the trap corresponding to 2.00 s are determined to be 1.00×10^{12} cm^{-2} and 5.00×10^{-1} s^{-1}, respectively, while N_{t2} and e_{t2} of the trap corresponding to 667 s are determined to be 1.00×10^{12} cm^{-2} and 5.00×10^{-4} s^{-1}, respectively. The obtained values are in good agreement with the values used in the simulation of the transient discharge current. This indicates that N_{ti} and e_{ti} can be determined in a wide emission-rate range by changing e_{ref}, even when the measurement time range is limited.

D. Distinction among traps with close emission rates

It is demonstrated that e_{ref} in Eq. (8) is also useful when there are traps with close emission rates in the film. Figure 3 shows the transient discharge current, which is simulated assuming the following two kinds of traps. N_{t1} and e_{t1} of Trap1 are 3×10^{12} cm^{-2} and 0.05 s^{-1}, respectively, and N_{t2} and e_{t2} of Trap2 are 1×10^{12} cm^{-2} and 0.01 s^{-1}, respectively. In this case, e_{t2} is very close to e_{t1}. The value of S is 1 mm^2.

The full curve in Fig. 4 represents the DCTS signal with $e_{\mathrm{ref}}=0\ \mathrm{s}^{-1}$. In this case, only one peak is detected, and the peak discharge time and peak value are 22.5 s and 3.47×10^{12} cm^{-2}, respectively. From Eqs. (6) and (7), N_{t1} and e_{t1} are determined to be 3.47×10^{12} cm^{-2} and 4.44×10^{-2} s^{-1}, respectively. These obtained values are only a little different from N_{t1} and e_{t1} used in the simulation of the transient discharge current. In the figure, the broken and

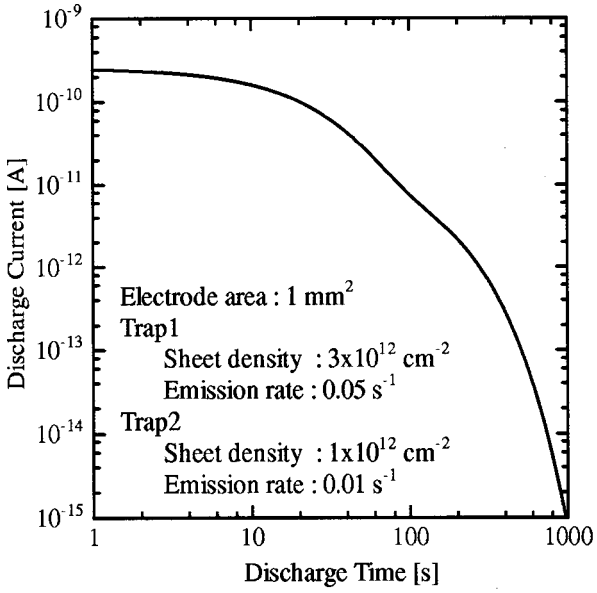

FIG. 3. Transient discharge current simulated assuming the following two kinds of traps. The sheet density and emission rate of Trap1 are 3×10^{12} cm^{-2} and 0.05 s^{-1}, respectively, and those of Trap2 are 1×10^{12} cm^{-2} and 0.01 s^{-1}, respectively.

chain curves, which correspond to Trap1 and Trap2, respectively, are simulated using the following equation:

$$N_{ti}e_{ti}t\exp[-(e_{ti}+e_{\mathrm{ref}})t+1]. \tag{17}$$

Since it is found that Trap1 mainly affects the DCTS signal with $e_{\mathrm{ref}}=0$ s^{-1}, it is reasonable that the values determined using the maximum of the DCTS signal are close to N_{t1} and e_{t1}, respectively.

The full curve in Fig. 5 represents the DCTS signal with $e_{\mathrm{ref}}=-0.0089$ s^{-1}. In this case, two peaks appear. One peak value is 4.35×10^{12} cm^{-2} at 29.4 s, and the other peak value is 9.09×10^{12} cm^{-2} at 910 s. From Eqs. (6) and (7), N_{t1} and

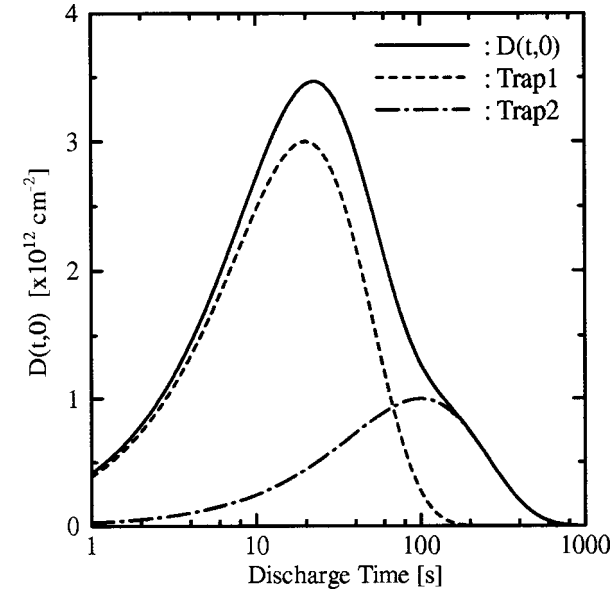

FIG. 4. DCTS signals with $e_{\mathrm{ref}}=0$ s^{-1} (full curve). The broken and chain curves are simulated using Eq. (17) for Trap1 and Trap2, respectively.

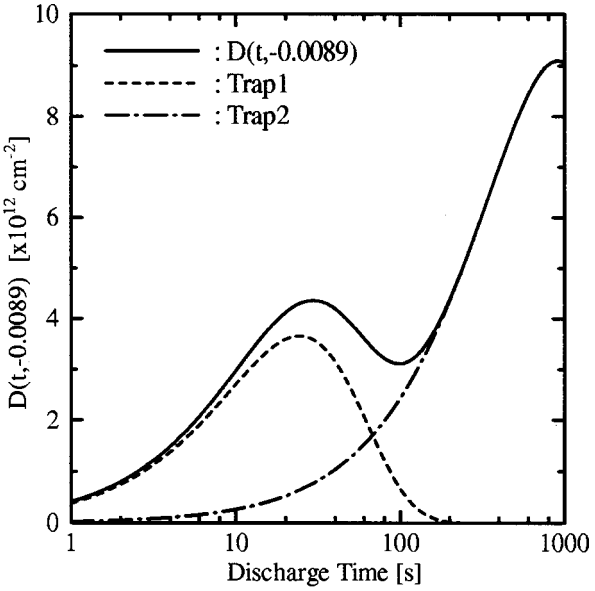

FIG. 5. DCTS signals with $e_{\mathrm{ref}}=-0.0089$ s^{-1} (full curve). The broken and chain curves are simulated using Eq. (17) for Trap1 and Trap2, respectively.

e_{t1} are determined to be 3.45×10^{12} cm^{-2} and 4.29×10^{-2} s^{-1}, respectively, while N_{t2} and e_{t2} are determined to be 9.99×10^{11} cm^{-2} and 1.00×10^{-2} s^{-1}, respectively. In the figure, the broken and chain curves, which are simulated using Eq. (17), correspond to Trap1 and Trap2, respectively. The peak corresponding to Trap2 is maximum when $e_{\mathrm{ref}}=-0.0089$ s^{-1}, although the peak corresponding to Trap1 is maximum when $e_{\mathrm{ref}}=0$ s^{-1}. Therefore, it is natural that the values determined using the maximum of the DCTS signal with $e_{\mathrm{ref}}=-0.0089$ s^{-1} are close to N_{t2} and e_{t2}, respectively.

Figure 6 shows the e_{ref} dependence of the peak value for Trap1 (the broken curve) or Trap2 (the chain curve). The peak corresponding to Trap1 is maximum when e_{ref}

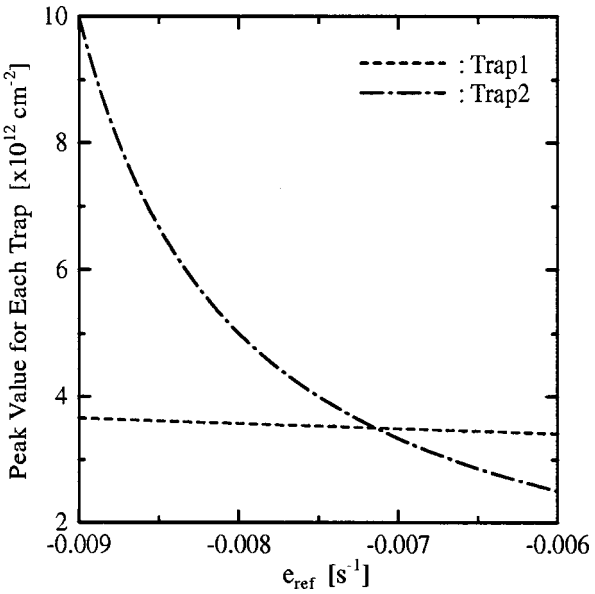

FIG. 6. The e_{ref} dependence of peak value for Trap1 (broken curve) or Trap2 (chain curve).

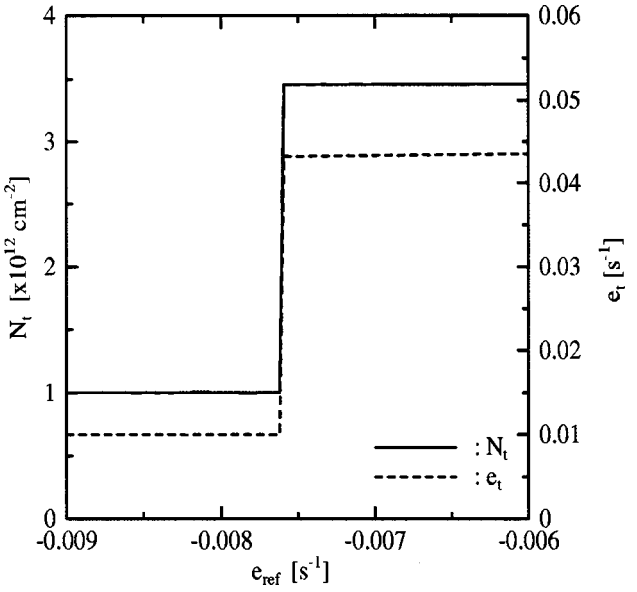

FIG. 7. The e_{ref} dependence of N_t or e_t determined from the maximum of the DCTS signal.

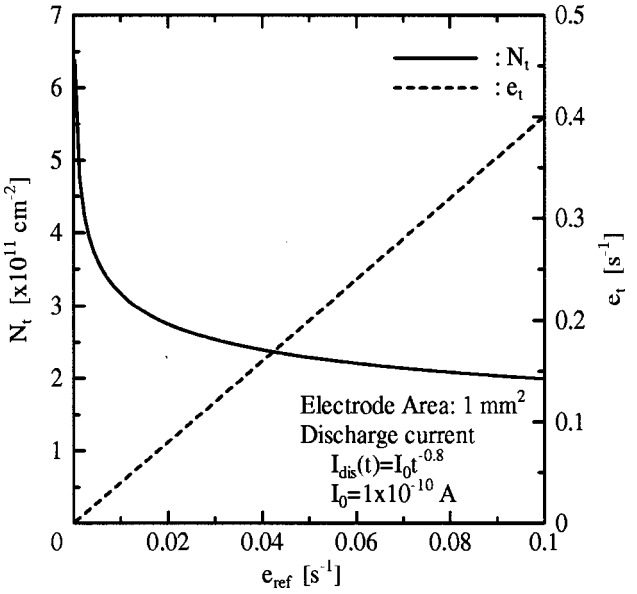

FIG. 8. The e_{ref} dependence of N_t or e_t determined from the maximum of the DCTS signal.

>-0.0071 s^{-1}, while the peak corresponding to Trap2 is maximum when $e_{ref}<-0.0071$ s^{-1}. This suggests that it is possible to distinguish between two traps using the e_{ref} dependence of N_t or e_t determined using the maximum of the DCTS signal.

Figure 7 shows the e_{ref} dependence of N_t or e_t determined from the maximum of the DCTS signal. The two discrete values of e_t or N_t clearly appear in the figure. Moreover, the obtained values are close to the values used in the simulation of the transient discharge current. Therefore, it is found that DCTS can distinguish among traps with close emission rates by changing e_{ref}.

E. Case of $I_{dis}(t)=I_0t^{-n}$

It is demonstrated that e_{ref} in Eq. (8) is useful when we distinguish between t^{-n} and a sum of $\exp(-e_{ti}t)$ with several close e_{ti}. The transient discharge currents in thin insulator films have often been reported to be approximately expressed as[27,28]

$$I_{dis}(t)=I_0t^{-n}, \tag{18}$$

where I_0 is the pre-exponential factor and $n>0$.

In the case of $n=1$, $D(t,e_{ref})$ increases monotonously with t when $e_{ref}<0$, while $D(t,e_{ref})$ decreases monotonously with t when $e_{ref}>0$. On the other hand, $D(t,e_{ref})$ is constant when $e_{ref}=0$. Therefore, there is no peak in the DCTS signal for any given e_{ref}.

In the case of $n>1$, $D(t,e_{ref})$ has a minimum when $e_{ref}<0$, while $D(t,e_{ref})$ decreases monotonously with t when $e_{ref}\geqslant 0$. Therefore, there is no peak in the DCTS signal for any given e_{ref}.

In the case of $0<n<1$, $D(t,e_{ref})$ increases monotonously with t when $e_{ref}\leqslant 0$, while $D(t,e_{ref})$ has a maximum when $e_{ref}>0$. Figure 8 shows the e_{ref} dependence of N_t or e_t obtained from the transient discharge current simulated using Eq. (18) with $I_0=1\times10^{-10}$ A and $n=0.8$. Although the DCTS signal has a maximum in this case, there are no discrete values of N_t or e_t determined using the maximum of the DCTS signal, as is clear from Fig. 8.

III. EXPERIMENT

Pt/PZT/Pt capacitors were used in our experiments. PZT thin films were deposited on Pt/SiO_2/(100)Si substrates at 570 °C by metalorganic chemical vapor deposition, using $Pb(C_2H_5)_4$, $Zr(O\text{-}t\text{-}C_4H_9)_4$ and $Ti(O\text{-}i\text{-}C_3H_7)_4$ as source precursors. The thickness of the PZT films was 200 nm. The area of the Pt top electrode was 0.79 mm^2. Details of the film preparation procedures were reported.[29,30]

DCTS measurements were performed at 373 K in an oxidation atmosphere ($Ar:O_2=1:1$ at 1 atom). The transient discharge current was measured at $V_{dis}=0$ V using a Keithley 236 source-measure unit, after V_{cha} of 2 V was applied to the capacitor in the interval of 600 s.

IV. RESULTS

Figure 9 shows the transient discharge current in the Pt/PZT/Pt capacitor. In order to search a peak of the DCTS signal precisely, the DCTS signal was calculated by interpolating $I_{dis}(t)$ with a cubic smoothing natural spline function. It should be noted that a peak of the DCTS signal is almost independent of a function type of interpolation when the DCTS signal is smooth because there is not a differential evaluation of the DCTS signal in the analysis.

Figure 10 shows the DCTS signal with $e_{ref}=0$ s^{-1}. The maximum discharge time and maximum value are 4.09 s and 1.54×10^{12} cm^{-2}, respectively. From Eqs. (6) and (7), N_t and e_t are determined to be 1.54×10^{12} cm^{-2} and 2.44×10^{-2} s^{-1}, respectively. In the case that the traps are uniformly distributed in the film, the trap density is estimated to be 7.70×10^{16} cm^{-3}, since the film thickness was 200 nm. The broken curve represents the signal simulated using Eq. (17) with the obtained values. Since the full curve is much

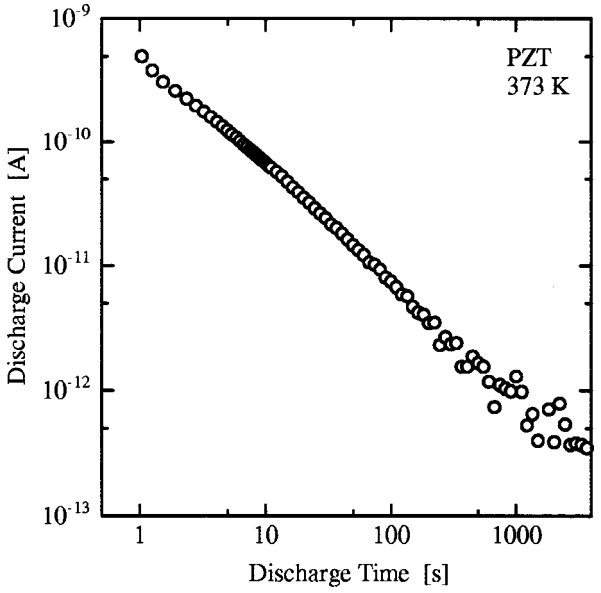

FIG. 9. Transient discharge current in Pt/PZT/Pt capacitor.

broader than the broken curve, the DCTS signal is considered to be affected by several traps with close emission rates.

Figure 11 shows the DCTS signal with $e_{\mathrm{ref}} = -0.000\,25\ \mathrm{s}^{-1}$. The maximum discharge time and maximum value are 1111 s and $1.60\times10^{12}\mathrm{cm}^{-2}$, respectively. From Eqs. (6) and (7), N_t and e_t are determined to be $1.25\times10^{12}\ \mathrm{cm}^{-2}$ and $1.15\times10^{-2}\ \mathrm{s}^{-1}$, respectively.

The broken curve represents the signal simulated using Eq. (17) with the obtained values. Since N_t and e_t for $e_{\mathrm{ref}} = -0.000\,25\ \mathrm{s}^{-1}$ are different from those for $e_{\mathrm{ref}} = 0\ \mathrm{s}^{-1}$, at least two kinds of traps with close emission rates are included in the PZT film.

Figure 12 shows the e_{ref} dependence of N_t (the full curve) or e_t (the broken curve) determined from the maximum of the DCTS signal at $e_{\mathrm{ref}}<0$. Three discrete values of e_t or N_t clearly appear in the figure. Moreover, the e_{ref} range of the constant N_t clearly corresponds one to one to the e_{ref} range of the constant e_t. Therefore, it is found that DCTS can distinguish among three kinds of traps (Trap1, Trap2 and Trap3) with close emission rates by changing negative e_{ref}. From Fig. 12, N_t and e_t of each trap can be determined; e_{t1} and N_{t1} of Trap1 are $1.15\times10^{-3}\ \mathrm{s}^{-1}$ and $1.2\times10^{12}\ \mathrm{cm}^{-2}$, respectively, and e_{t2} and N_{t2} of Trap2 are $1.39\times10^{-2}\ \mathrm{s}^{-1}$ and $1.53\times10^{12}\ \mathrm{cm}^{-2}$, respectively, and e_{t3} and N_{t3} of Trap3 are $2.3\times10^{-2}\ \mathrm{s}^{-1}$ and $1.54\times10^{12}\ \mathrm{cm}^{-2}$, respectively.

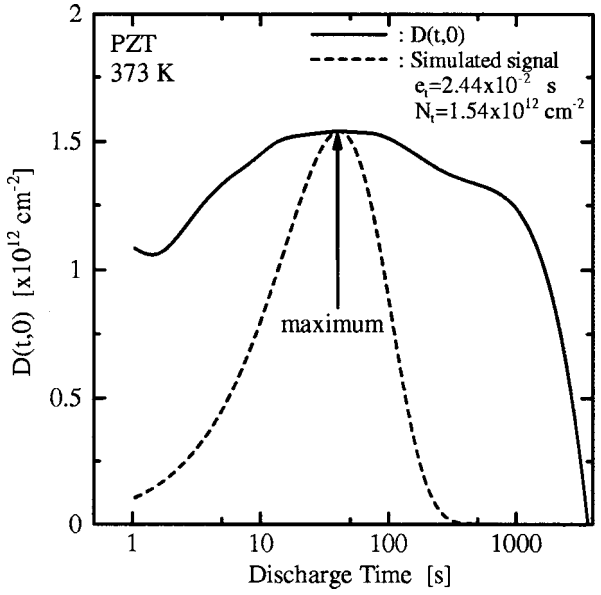

FIG. 10. DCTS signal (full curve) with $e_{\mathrm{ref}} = 0\ \mathrm{s}^{-1}$, which is calculated by interpolating $I_{\mathrm{dis}}(t)$ with a cubic smoothing natural spline function. The broken curve corresponds to the signal simulated using Eq. (17) with N_t and e_t determined from the maximum of the DCTS signal.

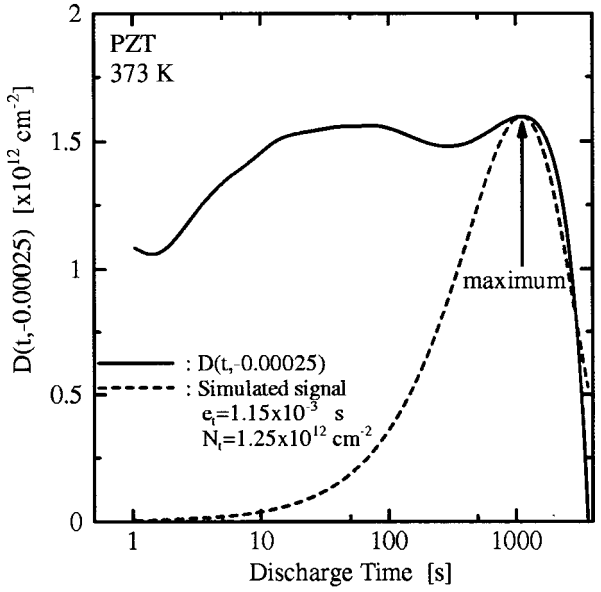

FIG. 11. DCTS signal (full curve) with $e_{\mathrm{ref}} = -0.000\,25\ \mathrm{s}^{-1}$. The broken curve corresponds to the signal simulated using Eq. (17) with N_t and e_t determined from the maximum of the DCTS signal.

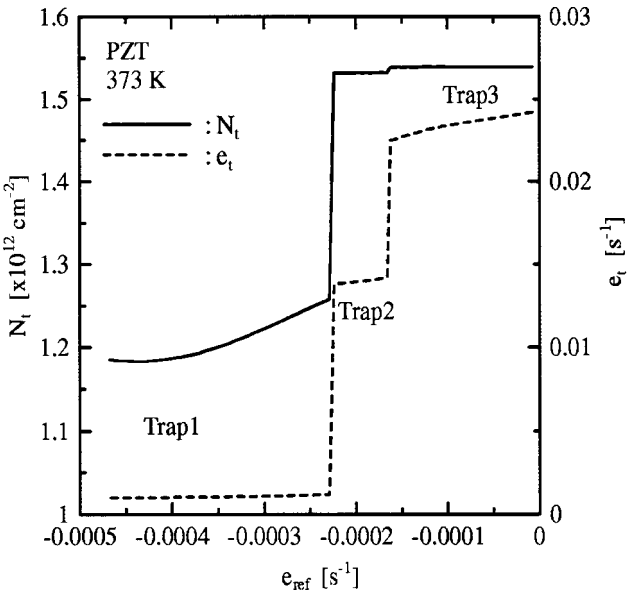

FIG. 12. The e_{ref} dependence of N_t (full curve) or e_t (broken curve) determined from the maximum of the DCTS signal at $e_{\mathrm{ref}}<0$.

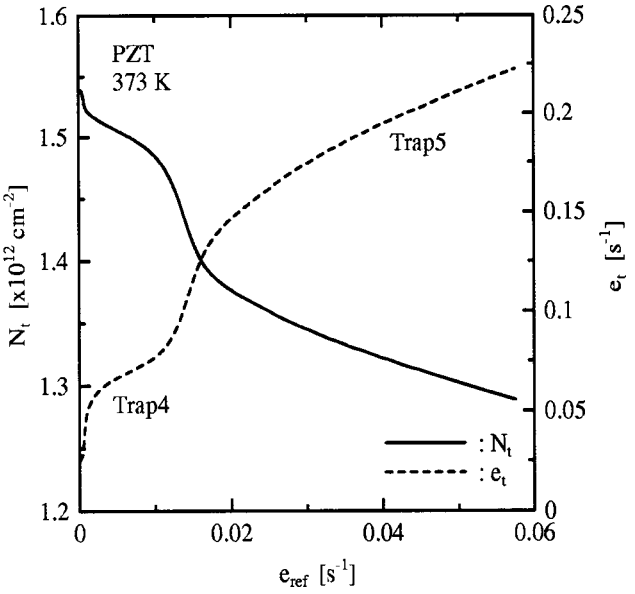

FIG. 13. The e_{ref} dependence of N_t (full curve) or e_t (broken curve) determined from the maximum of the DCTS signal at $e_{\mathrm{ref}} \geqslant 0$.

Figure 13 shows the e_{ref} dependence of N_t (the full curve) or e_t (the broken curve) determined from the maximum of the DCTS signal at $e_{\mathrm{ref}} \geqslant 0$. In addition to the three kinds of traps determined in Fig. 12, another two kinds of traps (Trap4 and Trap5) are considered to be included in this thin film. The e_{t4} and N_{t4} of Trap4 are 7.0×10^{-2} s^{-1} and 1.5×10^{12} cm^{-2}, respectively. On the other hand, the emission rate of Trap5 may be fluctuated, because both e_t and N_t of Trap5 change gradually with e_{ref} in the figure.

V. DISCUSSION

Using TSC, Wu and Sayer,[2] and Okino *et al.*[5] reported the trap density and trap level in PZT thin films. The TSC signal, $I_{\mathrm{TSC}}(T)$, is theoretically given by

$$I_{\mathrm{TSC}}(T) = qS\sum_{i=1} N_{ti}\nu_{ti}\exp\left[-\frac{\Delta E_{ti}}{kT} - \frac{\nu_{ti}}{\beta}\int_{T_0}^{T}\exp\left(-\frac{\Delta E_{ti}}{kT}\right)\mathrm{d}T\right] + I_{\mathrm{l}}(T), \tag{19}$$

where β is the heating rate, T_0 is the temperature at which heating is started, and $I_{\mathrm{l}}(T)$ is the steady-state leakage current at T. It should be noted that Eq. (19) is available only in the case of thermionic emission processes. Parameters for fitting a curve to the experimental $I_{\mathrm{TSC}}(T)$ are the sets of N_{ti}, ΔE_{ti} and ν_{ti}. In their analyses, since only one kind of trap was assumed, only three fitting parameters (N_{t1}, ΔE_{t1} and ν_{t1}) were used. The value of ΔE_{t1} was reported to be between 0.7 and 0.8 eV. The density was reported to be between 10^{18} and 10^{21} cm^{-3}, where traps were assumed to be uniformly distributed in the film. Moreover, since the trap density increased with switching cycles, the fatigues were considered to result from the increase of the trap density.[2,5]

The value of ν_{t1} is supposed to be between 10^7 s^{-1} and 10^8 s^{-1}, in order to fit a curve to their TSC signals. Using Eq. (9), e_{t1} is estimated to be on the order of 10^{-3} s^{-1} at 373 K. On the other hand, our e_t of five traps are between 1×10^{-3} and 7×10^{-2} s^{-1}. It is considered that TSC could not distinguish among the five traps with close emission rates determined by DCTS. Therefore, it has been clearly demonstrated that DCTS can distinguish among traps with close emission rates without any assumption of the number of traps.

VI. CONCLUSION

In order to investigate electrically active traps with close emission rates in thin insulator films precisely, DCTS has been proposed and tested. DCTS is superior to TSC as follows: (1) The DCTS measurements are carried out under an isothermal condition, indicating that it is not necessary to consider the influence of the pyroelectric currents as well as the temperature dependence of the steady-state leakage currents. (2) DCTS can distinguish among traps with close emission rates without any assumption of the number of trap species. (3) DCTS can determine the emission rates in the cases of any emission processes, while TSC is available only in the case of thermionic emission processes.

Moreover, DCTS is superior to the curve fitting of the transient discharge current at a constant temperature: (1) DCTS does not require us to assume the number of trap species, which is necessary to fit a curve to $I_{\mathrm{dis}}(t)$. (2) DCTS is easy to accurately determine the densities and emission rates of traps with close emission rates from the peaks of the signal, while the curve-fitting procedure is not.

Experimentally, we have illustrated that DCTS can determine the densities per unit area and emission rates of traps with five close emission rates in PZT thin films.

[1] J. F. Scott, *Ferroelectric Memories* (Springer, Berlin, 2000).
[2] Z. Wu and M. Sayer, *Proc. Eight IEEE Int. Symp. Applications of Ferroelectrics* (IEEE, Piscataway, NJ, 1994), p. 244.
[3] W. L. Warren, D. Dimos, B. A. Tuttle, R. D. Nasby, and G. E. Pike, Appl. Phys. Lett. **65**, 1018 (1994).
[4] W. L. Warren, G. E. Pike, B. A. Tuttle, and D. Dimos, Appl. Phys. Lett. **70**, 2010 (1997).
[5] H. Okino, Y. Toyoda, M. Shimizu, T. Horiuchi, T. Shiosaki, and K. Matsushige, Jpn. J. Appl. Phys., Part 1 **37**, 5137 (1998).
[6] D. V. Lang, J. Appl. Phys. **45**, 3023 (1974).
[7] H. Okushi and Y. Tokumaru, Jpn. J. Appl. Phys., Part 2 **19**, L335 (1980).
[8] H. Okushi, Philos. Mag. B **52**, 33 (1985).
[9] H. Matsuura, J. Appl. Phys. **64**, 1964 (1988).
[10] H. Matsuura and H. Okushi, *Amorphous & Microcrystalline Semiconductor Devices*, edited by J. Kanicki (Artech, Boston, 1992), Vol. II, p. 517.
[11] N. M. Johnson, D. J. Bartelink, and M. Schulz, *The Physics of SiO_2 and its Interfaces*, edited by S. T. Pantelides (Pergamon, New York, 1978), p. 421.
[12] A. Ricksand and O. Engstrom, J. Appl. Phys. **70**, 6915 (1991).
[13] R. R. Haering and E. N. Adams, Phys. Rev. **117**, 451 (1960).
[14] A. G. Milnes, *Deep Impurities in Semiconductor* (Wiley, New York, 1973), p. 226.
[15] H. Matsuura, M. Yoshimoto, and H. Matsunami, Jpn. J. Appl. Phys., Part 2 **34**, L185 (1995).
[16] H. Matsuura, M. Yoshimoto, and H. Matsunami, Jpn. J. Appl. Phys., Part 2 **34**, L371 (1995).
[17] H. Matsuura, Jpn. J. Appl. Phys., Part 1 **36**, 3569 (1997).
[18] H. Matsuura, Jpn. J. Appl. Phys., Part 1 **39**, 178 (2000).
[19] H. Matsuura, Jpn. J. Appl. Phys., Part 1 **39**, 2714 (2000).
[20] The Windows application software for DCTS can be freely downloaded from our web site (http://www.osakac.ac.jp/labs/matsuura/).
[21] H. Matsuura and K. Sonoi, Jpn. J. Appl. Phys., Part 2 **35**, L555 (1996).
[22] H. Matsuura, Jpn. J. Appl. Phys., Part 1 **36**, 3541 (1997).

[23] H. Matsuura, Y. Uchida, T. Hisamatsu, and S. Matsuda, Jpn. J. Appl. Phys., Part 1 **37**, 6034 (1998).
[24] H. Matsuura, T. Kimoto, and H. Matsunami, Jpn. J. Appl. Phys., Part 1 **38**, 4013 (1999).
[25] H. Matsuura, Y. Uchida, N. Nagai, T. Hisamatsu, T. Aburaya, and S. Matsuda, Appl. Phys. Lett. **76**, 2092 (2000).
[26] H. Matsuura, Y. Masuda, and S. Nishino, Jpn. J. Appl. Phys., Part 1 **39**, 5069 (2000).
[27] A. K. Jonscher, *Dielectric Relaxation in Solids* (Chelsea Dielectrics, London, 1983).
[28] R. Waser and D. M. Smyth, *Ferroelectric Thin Films: Synthesis and Basic Properties*, edited by C. P. Araujo, J. F. Scott, and G. E. Taylor (Gordon and Breach, Amsterdam, 1996), p. 73.
[29] M. Shimizu, H. Fujisawa, M. Sugiyama, and T. Shiosaki, Jpn. J. Appl. Phys., Part 1 **33**, 5135 (1994).
[30] M. Shimizu, M. Sugiyama, H. Fujisawa, and T. Shiosaki, Jpn. J. Appl. Phys., Part 1 **33**, 5167 (1994).